

Synchronization of Robot Manipulators Actuated By Induction Motors with Velocity Estimator

Felipe J. Torres^{1,*}, Gerardo V. Guerrero², Carlos D. García², Ricardo Zavala-Yoe³, Mario A. García¹ and Adolfo R. López⁴

Abstract: A complete modeling (including the actuator dynamics) of a robot manipulator that uses three-phase induction motors is presented in this paper. A control scheme is designed to synchronize robot manipulators actuated by induction motors under a master-slave scheme in the case where the joint velocity of the slave robots is estimated. All of the research on the synchronization of robot manipulators assumes the use of ideal actuators to drive the joints; for that reason, in this work, a three-phase induction motor is considered to be a direct-drive actuator for each joint. An entire model of the mated system is obtained by a combination of the dynamics of the induction motor and robot manipulator. Thus, the synchronization control algorithm for a master-slave scheme in both the joint space and workspace of robot manipulators driven by induction motors is developed. An observer based on the entire model is proposed to estimate the joint velocity of the slave robot manipulators. Through the Lyapunov criterion, a stability analysis of the synchronization control with a velocity estimator is detailed. The analytical results show the synchronization and estimation errors are globally, uniformly, and ultimately bounded. Simulations with multiple robots demonstrate the performance of the proposed control algorithm.

Keywords: Synchronization, robot manipulator, induction motor, Lyapunov stability, observer based on the model.

¹University of Guanajuato, Division of Engineering Campus Irapuato-Salamanca, Carretera Salamanca-Valle de Santiago km 3.5+1.8, Guanajuato, Salamanca, 36885, México.

²National Technological of Mexico/National Center of Research and Technological Development, Av. Palmira S/N colonia Palmira, Morelos, Cuernavaca, 62490, México.

³School of Engineering and Sciences, Monterrey Technological, Puente 222 Ejidos de Huipulco, Ciudad de México, 14380, México.

⁴Superior Technological Institute of Irapuato, Carretera Irapuato-Silao km 12.5, Guanajuato, Irapuato, 36821, México.

*Corresponding Author: Felipe J. Torres. Email: fdj.torres@ugto.mx.

1 Introduction

The controlled synchronization of robot manipulators has become a subject of interest within the scientific community during the last decade, mainly because of the efficiency and quality requirements in the production processes, in addition to the flexibility and maneuverability in the execution of tasks that a single robot cannot perform. This has led to the demand that two or more robots complete the same activity in a synchronized manner. This synchronization consists of matching two or more dynamic systems developing singly on a common trajectory from a certain instant onward, one of them called the master and the others the slaves.

In the literature, diverse algorithms of synchronization control have been stated, and all of these works assume ideal actuators. Thus, Nijmeijer et al. [Nijmeijer and Rodriguez-Angeles (2003)] applied a feedback control with access only to the robot's position. Chung et al. [Chung and Slotine (2009)], from contraction analysis, tracked a common trajectory while maintaining a formation through a directed graph of interconnection. Chopra et al. [Chopra and Spong (2008)] solved the previous features combined with constant delays of communications by using a passivity analysis. Abdessameud et al. [Abdessameud, Polushin and Tayebi (2014)] and Cicek et al. [Cicek and Dardemir (2018)] used a passivity theorem to consider varying delays. Nuno et al. [Nuño, Ortega, Jayawardhana et al. (2013)] considered the interconnection in the synchronization scheme as a non-directed graph.

Regarding the synchronization problems, different control algorithms have been applied; for instance, Zhang et al. [Zhang, Wang and Guo (2014)] required backstepping; Bouaziz et al. [Bouaziz, Bouteraa and Medhaffar (2013)] made use of cross-coupling; Mei et al. [Mei, Ren and Ma (2011)] used sliding mode controllers; and Chen et al. [Chen and Lewis (2011)] and Cui et al. [Cui and Yan (2012)] achieved synchronization through neural networks (NNs).

Moreover, synchronization approaches in the workspace have been reported. In the study by Kyrkjebø et al. [Kyrkjebø and Pettersen (2007)], in which a virtual manipulator to synchronize robot manipulators in a leader-follower scheme was used, the leader velocity was unknown. Liu et al. [Liu and Chopra (2012)] obtained the synchronization of heterogeneous robot manipulators with varying delays using the passivity property. Wang [Wang (2013)] synchronized robot manipulators without a leader, but rather used directed graphs strongly connected to develop an adaptable control law with attention to parametric uncertainties. Aldana et al. [Aldana, Nuño, Basañez et al. (2014)] synchronized the position and orientation of the robot manipulators: The position synchronization was designed with the use of the Jacobian, while the orientation was synchronized by means of the quaternions. Cicek et al. [Cicek, Dardemir and Zergeroglu (2015)] synchronized the end effectors of robot manipulators in both the joint space and workspace, considering the parametric uncertainties.

In practice, a great number of industrial robot manipulators use electric motors as actuators, where the DC-brushless permanent magnet (PMBLDC) servomotors are the most common. The advantage of PMBLDC motors is given by their relative ease control of the position and desired trajectory; however, their main disadvantage is cost, which is due to the use of rare

earths (neodymium-iron-boron or samarium-cobalt) in the manufacturing process of the permanent magnet and, furthermore, by the necessity of periodic mechanical maintenance. For this reason, an alternative to the use of servomotors is set by employing induction motors (IMs) as actuators. These devices generate a high-output torque and have a low manufacturing cost; furthermore, they are robust and can operate in any environmental conditions, while their disadvantage lies in their control difficulty, which is caused by their high non-linearity. Owing to this fact, Guerrero et al. [Guerrero-Ramírez and Tang (2001)] and Diniz et al. [de Diniz, Júnior, Honório et al. (2012)] researched robot manipulators driven by IMs only to track the desired trajectory.

A synchronization approach that considers ideal conditions in the joint space was addressed in Torres et al. [Torres, Guerrero, Garcia et al. (2016)], where robot manipulators are driven by IMs, and, consequently, the IMs were synchronized in the task execution as well. In this sense, Sun et al. [Sun, Gong, Yang et al. (2019)] synchronized multiple induction motors for a tracking system. In this work, the definition of the tracking error in relation to the angular velocity was considered. Therefore, it was necessary to avoid the chattering phenomena that might be depicted by noise in the velocity and acceleration measurements, leading to other problems in synchronization.

The objective of this work is to develop a master-slave synchronization control scheme for both the joint space and workspace of robot manipulators directly driven by IMs (designated as IM-Robot), considering the load torque for the IMs as the torque derived from the synchronization controller. Hence, the angular positions $q_i(t) \in \mathbb{R}^n$, as well as the position and orientation $\chi_i(t) \in \mathbb{R}^m$ of the i th slave IM-Robot are synchronized with respect to $q_j(t) \in \mathbb{R}^n$ and $\chi_j(t) \in \mathbb{R}^m$ of the master IM-Robot through the synchronization control approaches based on velocity observer, for the case in which only the angular position measurement of the joints of the slave IM-Robot is available.

The rest of this paper is organized as follows. Dynamic models of the robot manipulator and induction motor are presented in Section 2. In Section 3, the combination of IM dynamics and robot manipulator dynamics is depicted. In Section 4, the synchronization control designs with a velocity estimator in both the joint space and workspace are developed, and in Section 5, the results of the simulations are shown. Finally, conclusions are given in Section 6.

2 Dynamic models

2.1 Dynamic model of a robot manipulator

Consider p robot manipulators fully actuated in which the friction losses are neglected, with $k = 1, 2, \dots, n$ joints. The vector of the angular position of the robot joints is $q_i(t) \in \mathbb{R}^n$, $i = 1, 2, \dots, p$. Using the Euler-Lagrange formalism, the dynamic model of the i th robot is given by Behal et al. [Behal, Dixon, Dawson et al. (2009)]:

$$\mathbf{M}(q_i) \ddot{q}_i + \mathbf{C}(q_i, \dot{q}_i) \dot{q}_i + \mathbf{g}(q_i) = \tau_i, \quad (1)$$

where $\mathbf{M}(q) \in \mathbb{R}^{n \times n}$ is the inertia matrix, $\mathbf{C}(q, \dot{q}) \in \mathbb{R}^{n \times n}$ the Coriolis and centrifugal forces matrix, $\mathbf{g}(q) \in \mathbb{R}^n$ the vector of gravitational forces, and $\tau(t) \in \mathbb{R}^n$ the vector of

input torques. This model comprises the following properties:

1. The inertia matrix $\mathbf{M}(q) \in \mathbb{R}^{n \times n}$ is symmetric and positive definite for all $q_i \in \mathbb{R}^n$.
2. The matrix $\left[\dot{\mathbf{M}}_i(q_i) - 2\mathbf{C}_i(q_i, \dot{q}_i) \right]$ is skew-symmetric for all $x \in \mathbb{R}^n$,
 $x^T \left[\dot{\mathbf{M}}_i(q_i) - 2\mathbf{C}_i(q_i, \dot{q}_i) \right] x = 0$.

The position and orientation in the workspace of the end-effector of the i th robot manipulator are denoted by $\chi_i(t) \in \mathbb{R}^m$ through Cartesian coordinates:

$$\chi_i(t) = \begin{bmatrix} x_i(t) \\ y_i(t) \\ z_i(t) \end{bmatrix} = f(q_i), \quad (2)$$

where $f(\cdot) \in \mathbb{R}^m$ is a nonlinear function of the direct kinematics.

The relationships between the joint velocities $\dot{q}_i \in \mathbb{R}^n$ and the time derivative of the end-effector coordinates of the robot $\dot{\chi}_i \in \mathbb{R}^m$ in the workspace are given by

$$\dot{\chi}_i(t) = J_{ac}(q_i) \dot{q}_i, \quad (3)$$

where $J_{ac} \in \mathbb{R}^{m \times n}$ represents the Jacobian of the manipulator, defined as

$$J_{ac}(q_i) = \frac{\partial f(q_i)}{\partial q_i}. \quad (4)$$

The pseudo-inverse of $J_{ac} \in \mathbb{R}^{m \times n}$, described by $J_{ac}^+ \in \mathbb{R}^{n \times m}$, is defined as

$$J_{ac}^+ = J_{ac}^T (J_{ac} J_{ac}^T)^{-1}. \quad (5)$$

2.2 Dynamic model of IM

The vectors of the currents $i_\alpha - i_\beta$ and flows $\lambda_\alpha - \lambda_\beta$ of the stationary reference frame fixed to the stator $\alpha - \beta$ of the IM are used to express the equations in a field-oriented frame $d - q$. In this sense, the model of the IM mechanical and electrical dynamics without consideration of the effects of viscous friction is given by [Marino, Tomei and Verrelli (2010)]:

$$\begin{aligned} \frac{d\omega_m}{dt} &= \mu \lambda_d i_q - \frac{T_L}{J}, \\ \frac{d\lambda_d}{dt} &= -\alpha \lambda_d + \alpha L_m i_d, \\ \frac{di_d}{dt} &= -\gamma i_d + \alpha \beta \lambda_d + n_p \omega_m i_q + \alpha L_m \frac{i_q^2}{\lambda_d} + \frac{1}{\sigma L_s} u_d, \\ \frac{di_q}{dt} &= -\gamma i_q - \beta n_p \omega_m \lambda_d - n_p \omega_m i_d - \alpha L_m \frac{i_q i_d}{\lambda_d} + \frac{1}{\sigma L_s} u_q, \\ \frac{d\rho}{dt} &= n_p \omega_m + \alpha L_m \frac{i_q}{\lambda_d}, \end{aligned} \quad (6)$$

where $\rho = \arctan \frac{\lambda_\beta}{\lambda_\alpha}$, $\mu = \frac{3}{2} n_p \frac{L_m}{J L_r}$, $\alpha = \frac{R_r}{L_r}$, $\sigma = \left(1 - \frac{L_m^2}{L_s L_r}\right)$, $\beta = \frac{L_m}{\sigma L_s L_r}$, $\gamma = \frac{R_s L_r^2 + R_r L_m^2}{\sigma L_s L_r^2}$. ω_m is the rotor speed, i_d and i_q are the currents on the $d - q$ axes, and λ_d is the rotor flux linkage on the d axis. T_L and n_p are the load torque and number of pole pairs. J is the moment of inertia, which is defined as constant. L_m is the mutual inductance, and L_s and L_r are the self-inductances of the stator and rotor, respectively. f is the nominal frequency in (Hz). R_s and R_r are the resistances of the stator and rotor, respectively, in Ω . Finally, u_d and u_q are the non-linear state feedback control inputs, described by

$$\begin{bmatrix} u_d \\ u_q \end{bmatrix} = \sigma L_s \begin{bmatrix} -n_p \omega_m i_q - \alpha L_m \frac{i_q^2}{\lambda_d} - \alpha \beta \lambda_d + v_d \\ n_p \beta \omega_m \lambda_d + n_p \omega_m i_d + \alpha L_m \frac{i_d i_q}{\lambda_d} + v_q \end{bmatrix}. \quad (7)$$

Substitution of Eq. (7) into Eq. (6) results in the closed-loop system

$$\begin{aligned} \frac{d\omega_m}{dt} &= \mu \lambda_d i_q - \frac{T_L}{J}, \\ \frac{d\lambda_d}{dt} &= -\alpha \lambda_d + \alpha L_m i_d, \\ \frac{di_d}{dt} &= -\gamma i_d + v_d, \\ \frac{di_q}{dt} &= -\gamma i_q + v_q, \\ \frac{d\rho}{dt} &= n_p \omega_m + \alpha L_m \frac{i_q}{\lambda_d}, \end{aligned} \quad (8)$$

v_d and v_q are the new control inputs obtained by applying the next PI loops:

$$v_d = K_{d1} (\lambda_{dref} - \lambda_d) + K_{d2} \int (\lambda_{dref} - \lambda_d) dt, \quad (9)$$

$$v_q = K_{q1} (T_{ref} - T_{em}) + K_{q2} \int (T_{ref} - T_{em}) dt, \quad (10)$$

$$T_{ref} = K_{\tau1} (\omega_{ref} - \omega_m) + K_{\tau2} \int (\omega_{ref} - \omega_m) dt, \quad (11)$$

where λ_{dref} , T_{ref} and ω_{ref} are the references for rotor flux linkage, torque, and angular speed, respectively. K_{d1} , K_{d2} , K_{q1} , K_{q2} , $K_{\tau1}$ and $K_{\tau2}$ are the positive constant gains. T_{em} is the electromagnetic torque, defined as $T_{em} = \mu J \lambda_d i_q$.

3 Mated system: robot manipulator and induction motor

Consider that the k th joint, $k = 1, 2, \dots, n$, of each i th robot manipulator, $i = 1, 2, \dots, p$, being directly driven by an IM. It is also assumed that the amplitude of the flux linkage $\lambda_{d,ik}$ is regulated to the reference constant value $\lambda_{dref,ik}$ through the control loop Eq. (9);

hence, the closed-loop system for each IM is reduced to

$$\begin{aligned}
 J_{ik} \frac{d\omega_{m,ik}}{dt} &= \mu_{ik} J_{ik} \lambda_{dref,ik} i_{q,ik} - T_{L,ik}, \\
 \frac{di_{d,ik}}{dt} &= -\gamma_{ik} i_{d,ik} + v_{d,ik}, \\
 \frac{di_{q,ik}}{dt} &= -\gamma_{ik} i_{q,ik} + v_{q,ik}, \\
 \frac{d\rho_{ik}}{dt} &= n_p \omega_m + \alpha L_m \frac{i_{q,ik}}{\lambda_{dref,ik}}.
 \end{aligned} \tag{12}$$

Let $v_i = [v_{d,ik} \ v_{q,ik}]^T$, $I_i = [i_{d,ik} \ i_{q,ik}]^T$, $\Omega_i = [\omega_{m,i1}, \omega_{m,i2}, \dots, \omega_{m,in}]^T$, $T_{L,i} = [T_{L,i1}, T_{L,i2}, \dots, T_{L,in}]^T$, $\rho_i = [\rho_{i1}, \rho_{i2}, \dots, \rho_{in}]^T$, $J_i = \text{diag}[J_{i1}, J_{i2}, \dots, J_{in}]$, $B_i = \text{diag}[\mu_{i1} J_{i1}, \mu_{i2} J_{i2}, \dots, \mu_{in} J_{in}]$, $\Lambda_i = [\lambda_{dref,i1} i_{q,i1}, \lambda_{dref,i2} i_{q,i2}, \dots, \lambda_{dref,in} i_{q,in}]$, $\bar{\Gamma}_i = \left[\frac{i_{q,i1}}{\lambda_{dref,i1}}, \frac{i_{q,i2}}{\lambda_{dref,i2}}, \dots, \frac{i_{q,in}}{\lambda_{dref,in}} \right]$, $b_i = \text{diag}[\alpha_{i1} L_{m,i1}, \alpha_{i2} L_{m,i2}, \dots, \alpha_{in} L_{m,in}]$, where $\Omega_i, T_{L,i}, \Lambda_i \in \mathbb{R}^n$; $J_i, B_i \in \mathbb{R}^{n \times n}$.

The closed-loop reduced model representing all the k induction motors for the i th robot manipulator is expressed as

$$\begin{aligned}
 J_i \dot{\Omega}_i &= B_i \Lambda_i - T_{L,i}, \\
 \dot{I}_i &= -\gamma_i I_i + v_i, \\
 \dot{\varphi}_i &= n_{pi} \Omega_i + b_i \bar{\Gamma}_i,
 \end{aligned} \tag{13}$$

where $\dot{\Omega}_i = \frac{d\Omega_i}{dt} \in \mathbb{R}^n$.

The vector of the angular position $\theta_i \in \mathbb{R}^n$ from all the k induction motors for the i th robot manipulator is defined as

$$\theta_i = [\theta_{m,i1}, \theta_{m,i2}, \dots, \theta_{m,in}]^T.$$

To mate the robot manipulator dynamics and induction motor dynamics, we consider the following assumptions.

- ▲ **Assumption 1.** There exists a direct mechanical coupling between the rotor of the IM and the joint of the robot manipulator. This might reduce the periodical mechanical maintenance with respect to the PMBLDC motors; therefore,

$$q_i = \theta_i, \quad \dot{q}_i = \dot{\theta}_i = \Omega_i, \quad \ddot{q}_i = \ddot{\theta}_i = \dot{\Omega}_i. \tag{14}$$

- ▲ **Assumption 2.** The synchronization control law causes the input torque or required torque for each joint of the robot manipulator, which is considered as the load torque applied to each induction motor; thus,

$$T_{L,i} = \tau_i = M_i(q_i) \ddot{q}_i + C_i(q_i, \dot{q}_i) \dot{q}_i + g_i(q_i). \tag{15}$$

According to Assumption 2, it is possible to substitute Eq. (15) into Eq. (13); besides, Eq. (14) enables the state variables of the motor to equal those of the robot manipulator.

This gives

$$\begin{aligned}
J_i \dot{\Omega}_i &= B_i \Lambda_i - [M_i(q_i) \ddot{q}_i + C_i(q_i, \dot{q}_i) \dot{q}_i + g_i(q_i)], \\
B_i \Lambda_i &= J_i \ddot{q}_i + [M_i(q_i) \ddot{q}_i + C_i(q_i, \dot{q}_i) \dot{q}_i + g_i(q_i)], \\
B_i \Lambda_i &= [J_i + M_i(q_i)] \ddot{q}_i + C_i(q_i, \dot{q}_i) \dot{q}_i + g_i(q_i), \\
D_i(q_i) \ddot{q}_i + C_i(q_i, \dot{q}_i) \dot{q}_i + g_i(q_i) &= B_i \Lambda_i,
\end{aligned} \tag{16}$$

where $D_i(q_i) = J_i + M_i(q_i)$. The mated system is called IM-Robot.

This model has the same properties as listed in Section 2, because $\dot{D}_i(q_i) = \dot{J}_i + \dot{M}_i(q_i) = \dot{M}_i(q_i)$, remembering that J_i is a constant.

4 Synchronization control and velocity observer

4.1 Synchronization control in joint space

Synchronization errors $s_i, \dot{s}_i \in \mathbb{R}^n$ are defined as in [Rodriguez-Angeles and Nijmeijer (2004)]:

$$s_i = q_i - q_{ri}, \quad \dot{s}_i = \dot{q}_i - \dot{q}_{ri}. \tag{17}$$

The reference signals q_{ri} and $\dot{q}_{ri}, \ddot{q}_{ri}$ are established to consider the interactions between robots and ensure the synchronous behavior, as

$$\begin{aligned}
q_{ri} &= q_d - \sum_{j=1, j \neq i}^p K_{cp_i,j} (q_i - q_j), \\
\dot{q}_{ri} &= \dot{q}_d - \sum_{j=1, j \neq i}^p K_{cv_i,j} (\dot{q}_i - \dot{q}_j), \\
\ddot{q}_{ri} &= \ddot{q}_d - \sum_{j=1, j \neq i}^p K_{ca_i,j} (\ddot{q}_i - \ddot{q}_j),
\end{aligned} \tag{18}$$

where $q_d(t)$ is the common desired trajectory that each IM-Robot will be forced to track; $K_{cp_i,j}, K_{cv_i,j}, K_{ca_i,j} \in \mathbb{R}^{n \times n}$ are diagonal positive semi-definite matrices, and, for simplicity, it is assumed that they satisfy $K_{cp_i,j} = K_{cv_i,j} = K_{ca_i,j} = K_{i,j}$. Thus, from Eq. (14) and Eq. (18), the reference signals for the mated IM-Robot system are obtained:

$$\theta_{ref,i} = q_{ri}, \quad \omega_{ref,i} = \dot{q}_{ri}, \quad \dot{\omega}_{ref,i} = \ddot{q}_{ri}. \tag{19}$$

▲ Assumption 3. The torque necessary to achieve synchronization for each joint τ_i shall be the reference torque T_{ref} for the corresponding IM. This avoids the control loop PI Eq. (11) in the control scheme of the IM.

Taken from Torres et al. [Torres, Guerrero, Garcia et al. (2016)], the control law to achieve a master-slave synchronization of IM-Robot systems in the joint space is given by

$$B_i \Lambda_i = D_i(q_i) \ddot{q}_{ri} + C_i(q_i, \dot{q}_i) \dot{q}_{ri} + g_i(q_i) - K_{di} \dot{s}_i - K_{pi} s_i, \tag{20}$$

where K_{di} and K_{pi} are positive-definite gain matrices.

4.2 Synchronization control design in workspace

To attain synchronization of robot manipulators driven by IMs in the workspace, a controller design is given below, more details of which appear in Appendix A.

The position error in the workspace $e_i(t) \in \mathbb{R}^m$ is defined as

$$e_i = \chi_d - \chi_i. \quad (21)$$

The error dynamic equation is expressed as

$$\begin{aligned} \dot{e}_i &= \dot{\chi}_d - \dot{\chi}_i \\ &= \dot{\chi}_d - J_{ac}(q_i) \dot{q}_i \\ &= \dot{\chi}_d - J_{ac}(q_i) \dot{q}_i + \alpha e_i - \alpha e_i \\ &= -\alpha e_i + J_{ac} [J_{ac}^+ (\dot{\chi}_d + \alpha e_i) + (I_n - J_{ac}^+ J_{ac}) \vartheta_i - \dot{q}_i], \end{aligned} \quad (22)$$

where αe_i has been added and subtracted to facilitate the formulation of the control, $I_n \in \mathbb{R}^{n \times n}$ is the identity matrix, $\alpha \in \mathbb{R}^{m \times m}$ denotes a positive-definite gain matrix, and $\vartheta_i(t) \in \mathbb{R}^n$ is a signal constructed in accordance with the required control objective.

Based on the structure of Eq. (22), the filtered tracking error $r_i(\dot{\chi}_d, e_i, \dot{q}_i) \in \mathbb{R}^n$ is used to reduce the order of the error dynamic equation, which is defined as

$$r_i = J_{ac}^+ (\dot{\chi}_d + \alpha e_i) + (I_n - J_{ac}^+ J_{ac}) \vartheta_i - \dot{q}_i. \quad (23)$$

Thus, the position error of the IM-Robot system in the workspace could be written using $r_i(t) \in \mathbb{R}^n$ as

$$\dot{e}_i = -\alpha e_i + J_{ac} r_i. \quad (24)$$

The dynamics of the filtered tracking error is obtained by applying the time derivative of Eq. (23):

$$\dot{r}_i = \frac{d}{dt} [J_{ac}^+ (\dot{\chi}_d + \alpha e_i) + (I_n - J_{ac}^+ J_{ac}) \vartheta_i] - \ddot{q}_i. \quad (25)$$

Thus, the dynamic equation of the IM-Robot system in an open loop is written as

$$D_i(q_i) \dot{r}_i = -C_i(q_i, \dot{q}_i) r_i + Y_i \vartheta_i - B_i \Lambda_i, \quad (26)$$

where the regression matrix/parameters vector $Y_i \Phi_i$ is defined by

$$\begin{aligned} Y_i \Phi_i &= D_i(q_i) \frac{d}{dt} \{ J_{ac}^+ (\dot{\chi}_d + \alpha e_i) + (I_n - J_{ac}^+ J_{ac}) \vartheta_i \} \\ &\quad + C_i(q_i, \dot{q}_i) \left\{ \begin{array}{l} J_{ac}^+ (\dot{\chi}_d + \alpha e_i) \\ + (I_n - J_{ac}^+ J_{ac}) \vartheta_i \end{array} \right\} + g_i(q_i), \end{aligned} \quad (27)$$

where $Y_i(\ddot{\chi}_d, \dot{\chi}_d, \chi_i, q_i, \dot{q}_i, \vartheta_i, \dot{\vartheta}_i) \in \mathbb{R}^{n \times r}$ is the regression matrix, and $\Phi_i \in \mathbb{R}^r$ denotes the constant parameters of the system.

A candidate Lyapunov function is proposed to design the synchronization control in the workspace of IM-Robot systems:

$$V(r_i, e_i) = \sum_{i=1}^p \left\{ \frac{1}{2} r_i^T D_i(q_i) r_i + \frac{1}{2} e_i^T e_i \right\}. \quad (28)$$

The function $V(r_i, e_i)$ is positive-definite for all r_i, e_i and $V(r_i, e_i) = 0$ if and only if $r_i = 0, e_i = 0$.

The time derivative of the proposed Lyapunov function $V(r_i, e_i)$ is given by

$$\dot{V}(r_i, e_i) = \sum_{i=1}^p \left\{ r_i^T D_i(q_i) \dot{r}_i + \frac{1}{2} r_i^T \dot{D}_i(q_i) r_i + e_i^T \dot{e}_i \right\}. \quad (29)$$

By the skew-symmetric property of the $\left[\dot{D}_i(q_i) - 2C_i(q_i, \dot{q}_i) \right]$ matrix

$$\dot{V}(r_i, e_i) = \sum_{i=1}^p \left\{ -e_i^T \alpha e_i + r_i^T (Y_i \Phi_i - B_i \Lambda_i + J_{ac}^T e_i) \right\} \quad (30)$$

is obtained. An equality is established to achieve $\dot{V}(r_i, e_i) < 0$:

$$Y_i \Phi_i - B_i \Lambda_i + J_{ac}^T e_i = -K r_i, \quad (31)$$

where $K \in \mathbb{R}^{n \times n}$ is a constant positive-definite gain matrix.

Thus, $\dot{V}(r_i, e_i)$ is expressed as

$$\dot{V}(r_i, e_i) = - \sum_{i=1}^p \left\{ e_i^T \alpha e_i + r_i^T K r_i \right\} < 0. \quad (32)$$

In accordance with Behal et al. [Behal, Dixon, Dawson et al. (2009)], it is said the synchronization error e_i is global asymptotically stable.

A controller leading to master-slave synchronization of IM-Robot systems in the workspace is developed via Eq. (31) as

$$B_i \Lambda_i = Y_i \Phi_i + K r_i + J_{ac}^T e_i. \quad (33)$$

4.3 Joint variables estimator

Owing to the problems caused by the velocity measurements, an observer based on the model is used to estimate q_i and \dot{q}_i in the slave IM-Robot systems. Then, the stability analysis is developed. For more details, see Appendix B. Thus, the proposed observer is

$$\begin{aligned} \frac{d}{dt} \hat{q}_i &= \hat{\dot{q}}_i + \xi_1 \tilde{q}_i, \\ \frac{d}{dt} \hat{\dot{q}}_i &= -D_i^{-1}(q_i) \left[C_i(q_i, \hat{\dot{q}}_i) \hat{\dot{q}}_i + g_i(q_i) - B_i \Lambda_i + K_{pi} s_i + K_{di} \hat{s}_i \right] + \xi_2 \tilde{q}_i, \end{aligned} \quad (34)$$

where ξ_1 and ξ_2 are diagonal positive-definite matrices. The position estimation error $\tilde{q}_i \in \mathbb{R}^n$ and velocity estimation error $\tilde{\dot{q}}_i \in \mathbb{R}^n$ are given by

$$\begin{aligned} \tilde{q}_i &= q_i - \hat{q}_i, \\ \tilde{\dot{q}}_i &= \dot{q}_i - \hat{\dot{q}}_i. \end{aligned} \quad (35)$$

The estimation errors' dynamics is expressed as

$$\begin{aligned}\frac{d}{dt}\tilde{q}_i &= \dot{q}_i - \left(\hat{q}_i + \xi_1\tilde{q}_i\right) = \tilde{q}_i - \xi_1\tilde{q}_i, \\ \frac{d}{dt}\tilde{q}_i &= D_i^{-1}(q_i) [B_i\Lambda_i - C_i(q_i, \dot{q}_i)\dot{q}_i - g_i(q_i)] \\ &\quad + D_i^{-1}(q_i) \left[C_i(q_i, \hat{q}_i)\hat{q}_i + g_i(q_i) - B_i\Lambda_i + K_{pi}s_i + K_{di}\hat{s}_i \right] - \xi_2\tilde{q}_i.\end{aligned}\quad (36)$$

The candidate Lyapunov function for the stability analysis is proposed as

$$V_s(s_i, \dot{s}_i, \tilde{q}_i, \dot{\tilde{q}}_i) = V_1(s_i, \dot{s}_i) + V_2(\tilde{q}_i, \dot{\tilde{q}}_i), \quad (37)$$

where

$$V_1(s_i, \dot{s}_i) = \frac{1}{2}\dot{s}_i^T D_i(q_i) \dot{s}_i + \frac{1}{2}s_i^T K_{pi}s_i, \quad (38)$$

$$V_2(\tilde{q}_i, \dot{\tilde{q}}_i) = \frac{1}{2}\dot{\tilde{q}}_i^T P_1 \dot{\tilde{q}}_i + \frac{1}{2}\tilde{q}_i^T P_2 \tilde{q}_i.$$

P_1 and P_2 are diagonal positive-definite matrices. The time derivative of the proposed Lyapunov function is given separately by

$$\dot{V}_1(s_i, \dot{s}_i) = \dot{s}_i^T D_i(q_i) \ddot{s}_i + \frac{1}{2}\dot{s}_i^T \dot{D}_i(q_i) \dot{s}_i + s_i^T K_{pi}\dot{s}_i, \quad (39)$$

$$\dot{V}_2(\tilde{q}_i, \dot{\tilde{q}}_i) = \dot{\tilde{q}}_i^T P_1 \left(\frac{d}{dt}\tilde{q}_i\right) + \tilde{q}_i^T P_2 \left(\frac{d}{dt}\dot{\tilde{q}}_i\right). \quad (40)$$

The closed-loop error dynamic equation of the IM-Robot system is expressed as

$$D_i(q_i) \ddot{s}_i + C_i(q_i, \dot{q}_i) \dot{s}_i + K_{di}\dot{s}_i + K_{pi}s_i = 0. \quad (41)$$

The Lyapunov function derivative $\dot{V}_s(s_i, \dot{s}_i, \tilde{q}_i, \dot{\tilde{q}}_i)$ manifests an inequality given by

$$\begin{aligned}\dot{V}_s(s_i, \dot{s}_i, \tilde{q}_i, \dot{\tilde{q}}_i) &\leq -\dot{s}_i^T K_{di}\dot{s}_i - \begin{bmatrix} \tilde{q}_i \\ \dot{\tilde{q}}_i \end{bmatrix}^T \Delta \begin{bmatrix} \tilde{q}_i \\ \dot{\tilde{q}}_i \end{bmatrix} - \tilde{q}_i^T \varepsilon P_2 \xi_2 \tilde{q}_i \\ &\quad + \tilde{q}_i^T P_2 D_i^{-1}(q_i) \left(K_{pi}s_i + K_{di}\hat{s}_i \right),\end{aligned}\quad (42)$$

where

$$\Delta = \begin{bmatrix} P_1 \xi_1 & -P_1 \\ (1-\varepsilon) P_2 \xi_2 & P_2 D_i^{-1}(q_i) C_i(q_i, \tilde{q}_i) \end{bmatrix}, \quad 0 < \varepsilon < 1.$$

As of Eq. (42), the analysis is centered on the expression

$$-\tilde{q}_i^T \varepsilon P_2 \xi_2 \tilde{q}_i + \tilde{q}_i^T P_2 D_i^{-1}(q_i) \left(K_{pi}s_i + K_{di}\hat{s}_i \right)$$

as the cause of the non-negative definition of the Lyapunov function derivative, thus obtaining a factorization with respect to \tilde{q}_i^T :

$$\begin{aligned}-\tilde{q}_i^T \varepsilon P_2 \xi_2 \tilde{q}_i + \tilde{q}_i^T P_2 D_i^{-1}(q_i) \left(K_{pi}s_i + K_{di}\hat{s}_i \right) &= \\ -\tilde{q}_i^T \left[\varepsilon P_2 \xi_2 \tilde{q}_i - P_2 D_i^{-1}(q_i) \left(K_{pi}s_i + K_{di}\hat{s}_i \right) \right].\end{aligned}\quad (43)$$

This equation is ≤ 0 if and only if

$$|\tilde{q}_i| \geq \frac{D_i^{-1}(q_i) \left(K_{pi} s_i + K_{di} \hat{s}_i \right)}{\varepsilon \xi_2}. \quad (44)$$

Therefore, the Lyapunov function derivative is rewritten as

$$\dot{V}_s(s_i, \dot{s}_i, \tilde{q}_i, \dot{\tilde{q}}_i) \leq -\dot{s}_i^T K_{di} \dot{s}_i - \begin{bmatrix} \tilde{q}_i \\ \dot{\tilde{q}}_i \end{bmatrix}^T \Delta \begin{bmatrix} \tilde{q}_i \\ \dot{\tilde{q}}_i \end{bmatrix}, \quad (45)$$

$$\forall |\tilde{q}_i|, |\dot{\tilde{q}}_i| \geq \frac{D_i^{-1}(q_i) \left(K_{pi} s_i + K_{di} \hat{s}_i \right)}{\varepsilon \xi_2} = \vartheta.$$

Another condition for the negative definition of the Lyapunov function derivative is for the positive-definiteness of the matrix Δ to remain, which is ensured in accordance with Sylvester's criterion as

$$\begin{bmatrix} P_1 \xi_1 & -P_1 \\ (1-\varepsilon) P_2 \xi_2 & P_2 D_i^{-1}(q_i) C_i(q_i, \tilde{q}_i) \end{bmatrix} > 0 \quad (46)$$

if and only if

$$\frac{\xi_{1,m} D_{i,m}^{-1} C_{i,m}}{(1-\varepsilon) \xi_{2,M}} > 1, \quad (47)$$

where the sub-indexes m and M indicate the minimum and maximum matrix eigenvalues, respectively.

Definition 1. Letting $w_i = [s_i \ \dot{s}_i \ \tilde{q}_i \ \dot{\tilde{q}}_i]^T$ and the matrix

$$H_i = \begin{bmatrix} \frac{1}{2} K_{pi} & 1 & 1 & 1 \\ -1 & \frac{1}{2} D_i(q_i) & 1 & 1 \\ -1 & -1 & \frac{1}{2} P_1 & 1 \\ -1 & -1 & -1 & \frac{1}{2} P_2 \end{bmatrix}$$

the proposed Lyapunov function is rewritten as

$$\begin{aligned} V_s(w_i) &\geq w_i^T H_i w_i \geq \lambda_{\min}(H_i) w_i^2 \rightarrow \alpha_1(\kappa) \\ &= \lambda_{\min}(H_i) \kappa^2 \rightarrow \alpha_1(\varkappa) = \lambda_{\min}(H_i) \varkappa^2, \end{aligned} \quad (48)$$

$$\begin{aligned} V(w_i) &\leq w_i^T H_i w_i \leq \lambda_{\max}(H_i) w_i^2 \rightarrow \alpha_2(\kappa) \\ &= \lambda_{\max}(H_i) \kappa^2 \rightarrow \alpha_1(\varkappa) = \lambda_{\max}(H_i) \varkappa^2 \end{aligned} \quad (49)$$

In accordance with Khalil [Khalil (1996)], $w_i \leq \varkappa \Rightarrow V(w_i) \leq \alpha_2(\varkappa) = \varepsilon$. This ensures that

$$B_\mu \subset \Omega_\varepsilon = \{w_i : V_s(w_i) \leq \varepsilon\}.$$

Thus, $w_i \in \Omega_\varepsilon$ and the solutions are *GUUB* (globally uniformly ultimately bounded) by the bound

$$w_i \leq b = \alpha_1^{-1}(\alpha_2(\varkappa)) = \sqrt{\frac{\lambda_{\max}(H_i) \kappa^2}{\lambda_{\min}(H_i)}}. \quad (50)$$

Table 1: SCARA robot manipulator parameters (*BOSH*[®] *SR-8*)

Parameter	Value	Parameter	Value
l_1	0.43 m	m_1	15 kg
l_2	0.37 m	m_2	12 kg
l_{c1}	0.215 m	m_3	3 kg
l_{c2}	0.185 m	m_4	3 kg
I_1	0.2313 kg · m ²	I_2	0.1370 kg · m ²
$I_3 = I_4$	0.1007 kg · m ²	g	9.81 $\frac{m}{s^2}$

4.4 Synchronization control with velocity estimator

The synchronization control law of IM-Robot systems in the joint space with a velocity estimator of the slave IM-Robot is given by the expression

$$B_i \Lambda_i = D_i(q_i) \hat{\dot{q}}_{ri} + C_i(q_i, \hat{q}_i) \hat{q}_{ri} + g_i(q_i) - K_{di} \hat{s}_i - K_{pi} s_i. \quad (51)$$

In contrast, the synchronization control law of IM-Robot systems in the workspace with a velocity estimator of the slave IM-Robot is expressed as

$$B_i \Lambda_i = \hat{Y}_i \Phi_i + K \hat{r}_i + J_{ac}^T e_i, \quad (52)$$

where

$$\begin{aligned} \hat{r}_i &= J_{ac}^+ (\dot{\chi}_d + \alpha e_i) + (I_n - J_{ac}^+ J_{ac}) \vartheta_i - \hat{q}_i, \\ \hat{Y}_i \Phi_i &= D_i(q_i) \frac{d}{dt} \left\{ J_{ac}^+ (\dot{\chi}_d + \alpha e_i) + (I_n - J_{ac}^+ J_{ac}) \vartheta_i \right\} \\ &\quad + C_i(q_i, \hat{q}_i) \left\{ \begin{array}{l} J_{ac}^+ (\dot{\chi}_d + \alpha e_i) + \\ (I_n - J_{ac}^+ J_{ac}) \vartheta_i \end{array} \right\} + g_i(q_i). \end{aligned} \quad (54)$$

5 Simulation results

With the intention of proving the proposed synchronization approaches, robot manipulators of type SCARA with $k = 4$ joints driven by IMs were simulated in a scheme shown in Fig. (1) with one master IM-Robot system and three slave IM-Robot systems. The robot parameters are shown in Tab. 1, taken from the *BOSH*[®] *SR-8* datasheet. The parameters for each of the IMs appear in Tab. 2. Simulations were carried out on the *Simulink*[®] platform through the S-function level-2 with ode-45 solver, variable-step, and a simulation time of 10 s. The voltage sources can supply the required levels in the simulation settings.

5.1 IM-Robot synchronization in joint space

The desired trajectory in the joint space is described by the expression

$$q_d(t) = q_{din} + \left(\frac{q_{df} - q_{din}}{2} \right) \left[1 - \cos \left(\frac{\pi t}{t_f} \right) \right], \quad (55)$$

The gain matrices for the synchronization controller in the joint space are set as

$$\begin{aligned} K_{pj} &= \text{diag} [140] & K_{dj} &= \text{diag} [60] & K_{pi} &= \text{diag} [140] \\ K_{di} &= \text{diag} [110] & K_{d1} &= \text{diag} [2000] & K_{d2} &= \text{diag} [8000] \\ K_{q1} &= \text{diag} [180] & K_{q2} &= \text{diag} [300] \end{aligned}$$

It should be noted that the process for gain tuning in relation to the proposed controller was guided based on our prior experience with these types of synchronization controllers, attending to the positive-definite gain matrices.

The simulation results of the IM-Robot synchronization in the joint space for each slave IM-Robot are shown in Figs. 2-4. A solid line denotes the master IM-Robot trajectory, and a dashed line the slave IM-Robot system. In Fig. 5, all the trajectories are shown for each joint, including the desired trajectory. Synchronization errors and tracking error for each joint are displayed in Fig. 6, where $\zeta_{j,k}$ is the tracking error of the master IM-Robot with respect to the desired trajectory.

Remark 1. In the joint space, all the trajectories of the slave IM-Robot systems synchronize with the trajectory of the master IM-Robot system for each joint after an initial transient of 1.5 s, depending on the initial conditions. Therefore, the synchronization errors and the tracking error converge to zero in the case in which the velocity measurement is estimated.

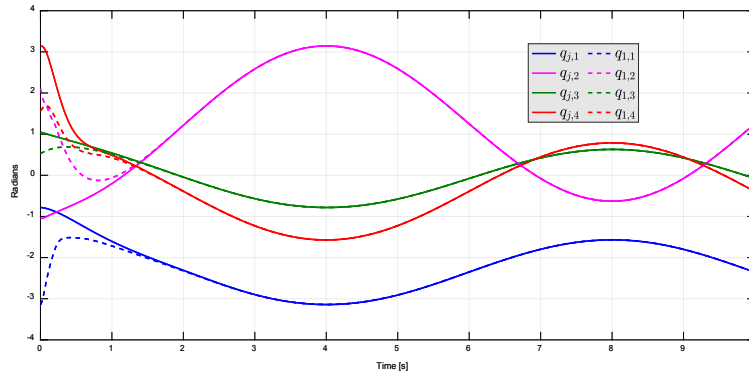


Figure 2: Synchronization in joint space of slave IM-Robot $i1$

5.2 IM-Robot synchronization in workspace

The desired trajectory in the workspace is described by

$$\chi_d(t) = [0.55 + 0.1 \sin(2t) \quad 0.3 + 0.1 \cos(2t) \quad 0.08t]^T \text{ m.} \quad (58)$$

The initial position of the master IM-Robot end-effector is set as

$$\chi(0)_j = [0.37 \quad 0.43 \quad 0]^T \text{ m.} \quad (59)$$

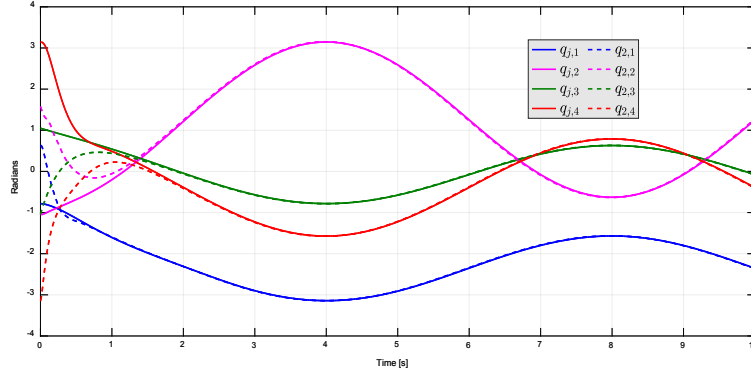


Figure 3: Synchronization in joint space of slave IM-Robot $i2$

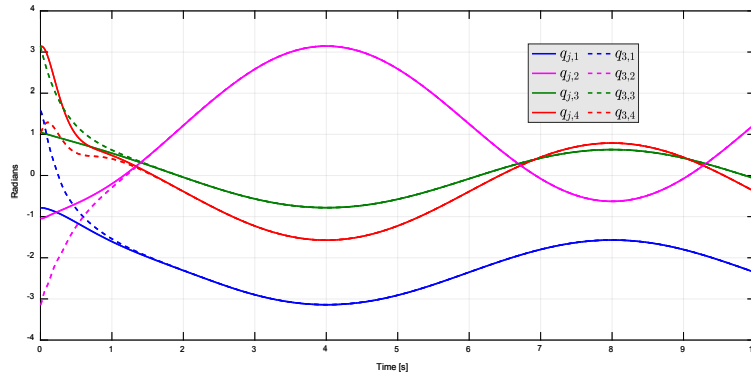


Figure 4: Synchronization in joint space of slave IM-Robot $i3$

For each slave IM-Robot, $i = 1, 2, 3$, and the initial position for the end-effector is established as

$$\chi(0)_i = \begin{bmatrix} \chi(0)_1 \\ \chi(0)_2 \\ \chi(0)_3 \end{bmatrix} = \begin{bmatrix} 0.2953 & 0.4235 & 0 \\ 0.4447 & 0.4235 & -0.1 \\ 0.2730 & 0.55 & -0.2 \end{bmatrix} \text{ m.} \quad (60)$$

The gain matrices used in the synchronization controller in the workspace are

$$\alpha = \text{diag} [250], \quad K = \text{diag} [30]. \quad (61)$$

The simulation results for IM-Robot synchronization in the workspace are presented as follows: In Fig. 7, the synchronization is seen in the $x - y$ plane; in Fig. 8, it is seen in the $x - z$ plane; finally, the workspace synchronization errors on the x and y axes are displayed in Fig. 9.

Remark 2. In the workspace, every position and orientation of the slave IM-Robot end-effectors synchronize with the position and orientation of the master IM-Robot end-effector

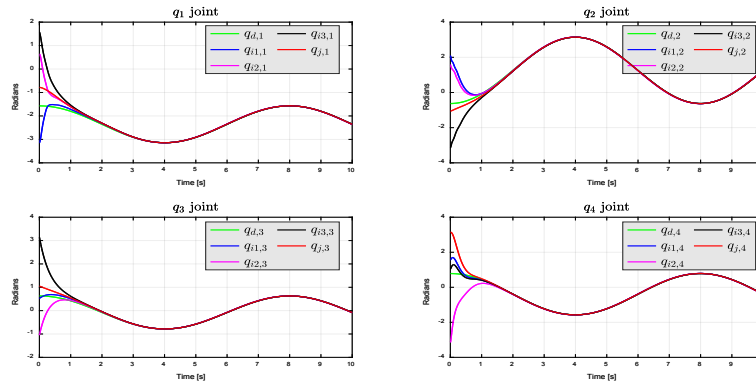


Figure 5: Synchronization in joint space of all IM-Robot slaves, each joint shown separately

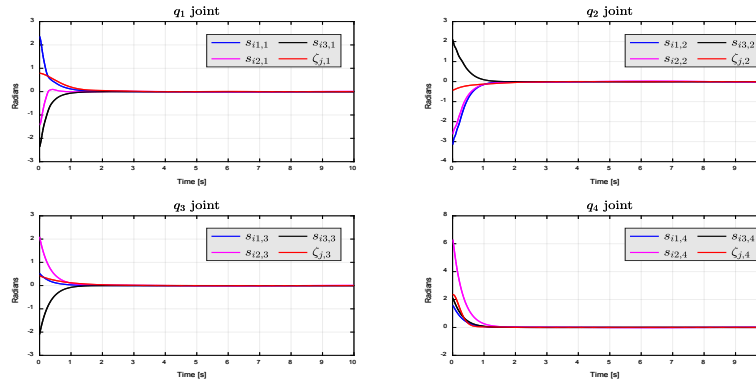


Figure 6: Synchronization error and tracking error in joint space of all IM-Robot slaves, each joint shown separately

while tracking a common desired trajectory. Furthermore, the synchronization errors converge to zero without velocity measurements.

The gain matrices for the velocity observer in both the joint space and workspace are established as

$$\xi_1 = \text{diag} [190], \quad \xi_2 = \text{diag} [200]. \quad (62)$$

Note that this choice of the gains satisfies the conditions given in Eq. (47) for each slave IM-Robot system in the scheme.

The position estimation error is shown in Fig. 10, and the velocity estimation position is presented in Fig. 11.

Remark 3. It is clear that the estimation errors converge to zero in both the joint space and workspace.

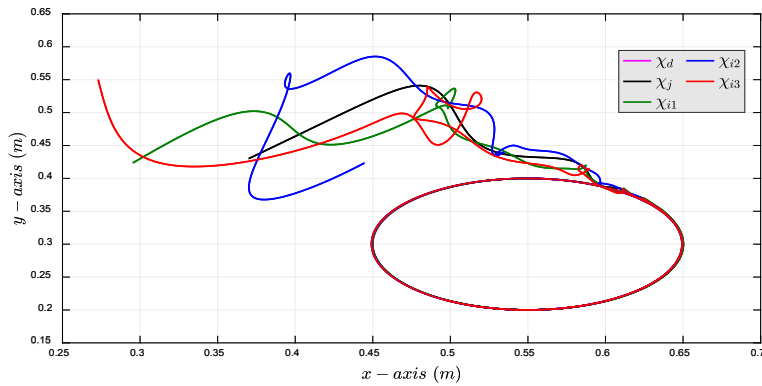


Figure 7: Synchronization in the workspace in the $x - y$ plane

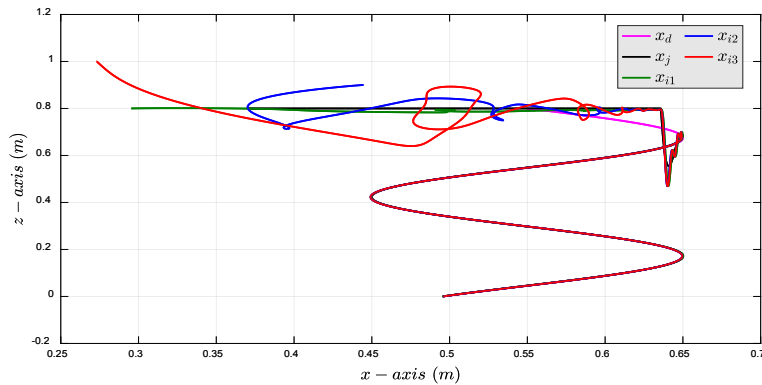


Figure 8: Synchronization in the workspace in the $x - z$ plane

6 Conclusions

The dynamics of the robot manipulator and IM have been combined to obtain the entire dynamic model of the mated IM-Robot system. Thus, a novel synchronization scheme including the actuator dynamics within the synchronization control with a velocity observer based on the entire IM-Robot model has been satisfactorily achieved, in both the joint space and workspace. Considering a direct mechanical coupling between the rotor of the IM and the joint of the robot manipulator, the proposed approach realizes synchronization of both the IM and robot manipulator.

The IM-Robot systems synchronize before tracking the desired trajectory, which is similar to the case in prior works in the literature in which ideal actuators were considered, so the use of an actuator with high nonlinear dynamics, like the IM, might allow reliable performance while minimizing costs.

Based on the results of Lyapunov analysis, the proposed velocity observer exhibited GUUB estimation closed-loop errors. The simulation results, assuming knowledge of the

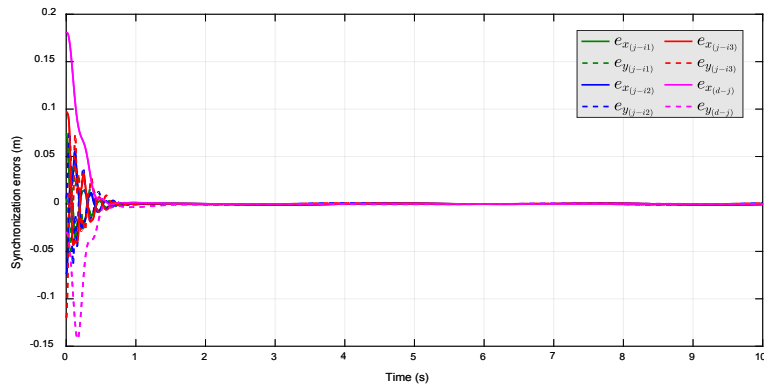


Figure 9: Synchronization errors in the workspace on the x and y axes

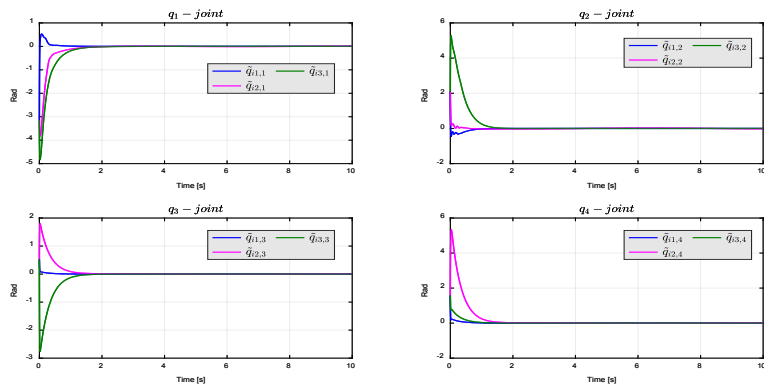


Figure 10: Position estimation error for the synchronization in joint space

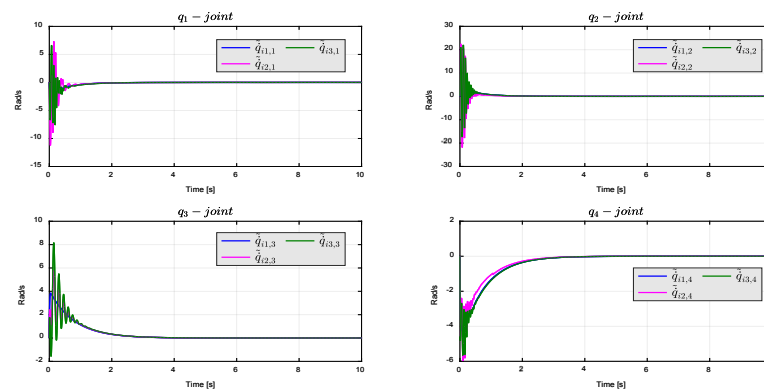


Figure 11: Velocity estimation error for the synchronization in the workspace

parameters and availability of the partial state and ideal sources in the simulations, show the feasibility of the proposed synchronization approach.

Future works will be directed at obtaining experimental results to compare the effects of chattering caused by the noise in the velocity measurements against the performance of the proposed observer. Moreover, future approaches will be undertaken that include time delays and parametric uncertainties.

Acknowledgement: This research was supported by University of Guanajuato-PFCE2019. We would also like to express our gratitude to the Department of Mechanical Engineering for supporting the academic resources needed for this work.

References

- Abdessameud, A.; Polushin, I. G.; Tayebi, A.** (2014): Synchronization of Lagrangian systems with irregular communication delays. *IEEE Transactions on Automatic Control*, vol. 59, no. 1, pp. 187-193.
- Aldana, C. I.; Nuño, E.; Basañez, L.; Romero, E.** (2014): Operational space consensus of multiple heterogeneous robots without velocity measurements. *Journal of the Franklin Institute*, vol. 351, no. 3, pp. 1517-1539.
- Behal, A.; Dixon, W.; Dawson, D. M.; Xian, B.** (2009): Lyapunov-based control of robotic systems. *CRC Press*, vol. 36.
- Bouaziz, F. A.; Bouteraa, Y.; Medhaffar, H.** (2013): Distributed sliding mode control of cooperative robotic manipulators. *10th International Multi-Conference on Systems, Signals & Devices*, pp. 1-7.
- Chen, G.; Lewis, F. L.** (2011): Distributed adaptive tracking control for synchronization of unknown networked Lagrangian systems. *IEEE Transactions on Systems, Man, and Cybernetics, Part B (Cybernetics)*, vol. 41, no. 3, pp. 805-816.
- Chopra, N.; Spong, M. W.** (2008): Output synchronization of nonlinear systems with relative degree one. *Recent Advances in Learning and Control*, pp. 51-64.
- Chung, S. J.; Slotine, J. J. E.** (2009): Cooperative robot control and concurrent synchronization of Lagrangian systems. *IEEE Transactions on Robotics*, vol. 25, no. 3, pp. 686-700.
- Cicek, E.; Dasdemir, J.** (2018): Adaptive output-feedback synchronisation of electromechanical systems under time-varying communication delays. *International Journal of Control*, pp. 1-12.
- Cicek, E.; Dasdemir, J.; Zergeroglu, E.** (2015): Coordinated synchronization of multiple robot manipulators with dynamical uncertainty. *Transactions of the Institute of Measurement and Control*, vol. 37, no. 5, pp. 672-683.
- Cui, R.; Yan, W.** (2012): Mutual synchronization of multiple robot manipulators with unknown dynamics. *Journal of Intelligent & Robotic Systems*, vol. 68, no. 2, pp. 105-119.
- de Diniz, E.; Júnior, A. B.; Honório, D. A.; Barreto, L. H.; Dos Reis, L. L.** (2012): An elbow planar manipulator driven by induction motors using sliding mode control for current loop. *Control and Cybernetics*, vol. 41, no. 2, pp. 395-413.

- Guerrero-Ramírez, G.; Tang, Y.** (2001): Motion control of rigid robots driven by current-fed induction motors. *Mechatronics*, vol. 11, no. 1, pp. 13-25.
- Khalil, H. K.** (1996): *Nonlinear Systems*. Prentice-Hall, New Jersey.
- Kyrkjebo, E.; Pettersen, K. Y.** (2007): Operational space synchronization of two robot manipulators through a virtual velocity estimate. *Decision and Control, 46th IEEE Conference on*, pp. 1052-1057.
- Liu, Y.-C.; Chopra, N.** (2012): Controlled synchronization of heterogeneous robotic manipulators in the task space. *IEEE Transactions on Robotics*, vol. 28, no. 1, pp. 268-275.
- Marino, R.; Tomei, P.; Verrelli, C. M.** (2010): *Induction Motor Control Design*. Springer Science & Business Media.
- Mei, J.; Ren, W.; Ma, G.** (2011): Distributed coordinated tracking with a dynamic leader for multiple Euler-Lagrange systems. *IEEE Transactions on Automatic Control*, vol. 56, no. 6, pp. 1415-1421.
- Nijmeijer, H.; Rodriguez-Angeles, A.** (2003): Synchronization of mechanical systems. *World Scientific*, vol. 46.
- Nuño, E.; Ortega, R.; Jayawardhana, B.; Basañez, L.** (2013): Coordination of multi-agent Euler-Lagrange systems via energy-shaping: networking improves robustness. *Automatica*, vol. 49, no. 10, pp. 3065-3071.
- Rodriguez-Angeles, A.; Nijmeijer, H.** (2004): Mutual synchronization of robots via estimated state feedback: a cooperative approach. *IEEE Transactions on Control Systems Technology*, vol. 12, no. 4, pp. 542-554.
- Sun, C.; Gong, G.; Yang, H.; Wang, F.** (2019): Fuzzy sliding mode control for synchronization of multiple induction motors drive. *Transactions of the Institute of Measurement and Control*, vol. 41, no. 11, pp. 3223-3234.
- Torres, F. J.; Guerrero, G. V.; Garcia, C. D.; Gomez, J. F.; Adam, M. et al.** (2016): Master-slave synchronization of robot manipulators driven by induction motors. *IEEE Latin America Transactions*, vol. 14, no. 9, pp. 3986-3991.
- Wang, H.** (2013): Passivity based synchronization for networked robotic systems with uncertain kinematics and dynamics. *Automatica*, vol. 49, no. 3, pp. 755-761.
- Zhang, W.; Wang, Z.; Guo, Y.** (2014): Backstepping-based synchronisation of uncertain networked Lagrangian systems. *International Journal of Systems Science*, vol. 45, no. 2, pp. 145-158.

Appendix A.

In this appendix, the design of the synchronization controller in the workspace is presented in detail as follows. From the Eq. (25), it is multiplied by the inertia matrix $D_i(q_i)$ of the matched IM-Robot system, then substitution of the IM-Robot dynamics results in the expression:

$$\begin{aligned} D_i(q_i) \dot{r}_i &= D_i(q_i) \left\{ \frac{d}{dt} \begin{bmatrix} J_{ac}^+ (\dot{\chi}_d + \alpha e_i) \\ + (I_n - J_{ac}^+ J_{ac}) \vartheta_i \end{bmatrix} \right\} - D_i(q_i) \ddot{q}_i \\ &= D_i(q_i) \left\{ \frac{d}{dt} \begin{bmatrix} J_{ac}^+ (\dot{\chi}_d + \alpha e_i) \\ + (I_n - J_{ac}^+ J_{ac}) \vartheta_i \end{bmatrix} \right\} + C_i(q_i, \dot{q}_i) \dot{q}_i + g_i(q_i) - B_i \Lambda_i. \end{aligned} \quad (63)$$

To reconstruct the structure of Eq. (23), $C_i(q_i, \dot{q}_i) [J_{ac}^+ (\dot{\chi}_d + \alpha e_i) + (I_n - J_{ac}^+ J_{ac}) \vartheta_i]$ is added and subtracted to Eq. (63), which gives

$$\begin{aligned} D_i(q_i) \dot{r}_i &= D_i(q_i) \left\{ \frac{d}{dt} \begin{bmatrix} J_{ac}^+ (\dot{\chi}_d + \alpha e_i) \\ + (I_n - J_{ac}^+ J_{ac}) \vartheta_i \end{bmatrix} \right\} + C_i(q_i, \dot{q}_i) \dot{q}_i + g_i(q_i) - B_i \Lambda_i \\ &\quad + C_i(q_i, \dot{q}_i) \begin{bmatrix} J_{ac}^+ (\dot{\chi}_d + \alpha e_i) \\ + (I_n - J_{ac}^+ J_{ac}) \vartheta_i \end{bmatrix} - C_i(q_i, \dot{q}_i) \begin{bmatrix} J_{ac}^+ (\dot{\chi}_d + \alpha e_i) \\ + (I_n - J_{ac}^+ J_{ac}) \vartheta_i \end{bmatrix}. \end{aligned} \quad (64)$$

Substitution of Eq. (26) into Eq. (29) results as

$$\begin{aligned} \dot{V}(r_i, e_i) &= \sum_{i=1}^p \left\{ \begin{array}{l} r_i^T (-C_i(q_i, \dot{q}_i) r_i + Y_i \Phi_i - B_i \Lambda_i) \\ + \frac{1}{2} r_i^T \dot{D}_i(q_i) r_i + e_i^T (-\alpha e_i + J_{ac} r_i) \end{array} \right\} \\ &= \sum_{i=1}^p \left\{ \begin{array}{l} r_i^T \left(\frac{1}{2} \dot{D}_i(q_i) - C_i(q_i, \dot{q}_i) \right) r_i - e_i^T \alpha e_i \\ + r_i^T (Y_i \Phi_i - B_i \Lambda_i + J_{ac}^T e_i) \end{array} \right\}. \end{aligned} \quad (65)$$

Appendix B.

This appendix shows details of the stability analysis of the proposed observer given in Eq. (34).

Substitution of Eq. (41) into Eq. (39) results as

$$\begin{aligned} \dot{V}_1(s_i, \hat{s}_i) &= \dot{s}_i^T [-C_i(q_i, \dot{q}_i) \hat{s}_i - K_{di} \hat{s}_i - K_{pi} s_i] + \frac{1}{2} \dot{s}_i^T \dot{D}_i(q_i) \hat{s}_i + s_i^T K_{pi} \hat{s}_i \\ &= \dot{s}_i^T \left[\frac{1}{2} \dot{D}_i(q_i) \hat{s}_i - C_i(q_i, \dot{q}_i) \hat{s}_i \right] - \dot{s}_i^T K_{di} \hat{s}_i - \dot{s}_i^T K_{pi} s_i + s_i^T K_{pi} \hat{s}_i \\ &= -\dot{s}_i^T K_{di} \hat{s}_i. \end{aligned} \quad (66)$$

Substitution of Eq. (36) into Eq. (40) gives

$$\begin{aligned} \dot{V}_2(\tilde{q}_i, \tilde{\dot{q}}_i) &= \tilde{q}_i^T P_1 (\tilde{q}_i - \xi_1 \tilde{q}_i) + \tilde{q}_i^T P_2 \left\{ D_i^{-1}(q_i) \begin{bmatrix} -C_i(q_i, \tilde{q}_i) \tilde{q}_i \\ + K_{pi} s_i + K_{di} \hat{s}_i \end{bmatrix} - \xi_2 \tilde{q}_i \right\} q_i \\ &= \tilde{q}_i^T P_1 \tilde{q}_i - \tilde{q}_i^T P_1 \xi_1 \tilde{q}_i - \tilde{q}_i^T P_2 D_i^{-1}(q_i) C_i(q_i, \tilde{q}_i) \tilde{q}_i \\ &\quad + \tilde{q}_i^T P_2 D_i^{-1}(q_i) K_{pi} s_i + \tilde{q}_i^T P_2 D_i^{-1}(q_i) K_{di} \hat{s}_i - \tilde{q}_i^T P_2 \xi_2 \tilde{q}_i. \end{aligned} \quad (67)$$

Therefore,

$$\begin{aligned} \dot{V}_s(s_i, \dot{s}_i, \tilde{q}_i, \dot{\tilde{q}}_i) = & -\dot{s}_i^T K_{di} \dot{s}_i + \tilde{q}_i^T P_1 \dot{\tilde{q}}_i - \tilde{q}_i^T P_1 \xi_1 \tilde{q}_i - \tilde{q}_i^T P_2 D_i^{-1}(q_i) C_i(q_i, \tilde{q}_i) \tilde{q}_i \\ & + \tilde{q}_i^T P_2 D_i^{-1}(q_i) K_{pi} s_i + \tilde{q}_i^T P_2 D_i^{-1}(q_i) K_{di} \hat{s}_i - \tilde{q}_i^T P_2 \xi_2 \tilde{q}_i. \end{aligned} \quad (68)$$

Considering a matrix representation,

$$\begin{aligned} \dot{V}_s(s_i, \dot{s}_i, \tilde{q}_i, \dot{\tilde{q}}_i) = & -\dot{s}_i^T K_{di} \dot{s}_i - \begin{bmatrix} \tilde{q}_i \\ \dot{\tilde{q}}_i \end{bmatrix}^T Z \begin{bmatrix} \tilde{q}_i \\ \dot{\tilde{q}}_i \end{bmatrix} + \tilde{q}_i^T P_2 D_i^{-1}(q_i) K_{pi} s_i \\ & + \tilde{q}_i^T P_2 D_i^{-1}(q_i) K_{di} \hat{s}_i, \end{aligned} \quad (69)$$

where $Z = \begin{bmatrix} P_1 \xi_1 & -P_1 \\ P_2 \xi_2 & P_2 D_i^{-1}(q_i) C_i(q_i, \tilde{q}_i) \end{bmatrix}$.

The expression $\tilde{q}_i^T \varepsilon P_2 \xi_2 \tilde{q}_i$ is added and subtracted to Eq. (69), with $0 < \varepsilon < 1$, where the time derivative of the Lyapunov function $\dot{V}_s(s_i, \dot{s}_i, \tilde{q}_i, \dot{\tilde{q}}_i)$ manifests an inequality given by Eq. (42).